Available online at www.sciencedirect.com
ScienceDirect
Journal of the European Ceramic Society 28 (2008) 2405–2410
www.elsevier.com/locate/jeurceramsoc

Nanoparticulate composites of melt textured $YBa_2Cu_3O_{7-x}$ superconductors

Oratai Jongprateep, Fatih Dogan *

Missouri University of Science and Technology, Department of Materials Science and Engineering, 222 McNutt Hall, Rolla, MO 65409, USA

Available online 7 March 2008

Abstract

It has been shown that $Nd_{1+x}Ba_{2-x}Cu_3O_{7-x}$ could exhibit a pronounced $J_c(H)$ peak effect, which results in an enhancement of the critical current density under the medium range magnetic field. Additions of small quantities of Nd_2O_3 into Pt-doped $YBa_2Cu_3O_{7-x}$ (Y123) resulted in the formation of nanosized (30–60 nm) secondary phases which are expected to have a significant effect on superconducting properties of melt textured Y123 single crystals. By considering of solidification kinetics, effect of neodymium oxide and platinum addition on processing parameters of melt textured Y123 superconductors are discussed.

Keywords: Oxide superconductors; Superconductivity; Inclusions; Interfaces; Nano-sized particles

1. Introduction

(LRE)–Ba–Cu–O superconductors (where LRE is a light rare earth element such as Nd, Sm, Eu and Gd) have great potential for practical applications due to their ability to trap large magnetic fields. It has been reported that $NdBa_2Cu_3O_{7-x}$ (Nd123) exhibits a pronounced $J_c(H)$ peak effect, which results in an enhancement of the critical current density under medium and high magnetic fields.[1] However, a major problem for the use of Nd123 in applications is the sluggish and low superconducting transition temperatures caused by formation of solute solutions. Owing to a comparable ionic radius of Ba^{2+} and Nd^{3+}, Ba sites can be partially substituted by Nd^{3+} ions, which result in the formation of $Nd_{1+x}Ba_{2-x}Cu_3O_{7-\delta}$ solid solution.[2,3] The partial substitution of Ba^{2+} by Nd cations leads to depression of a hole or carrier concentration and thereby resulting in a low superconducting transition temperature, T_c.[4–8] In addition, difficulties in growing large Nd123 single crystals by conventional top-seeded melt texturing growth (TSMTG) technique are often encountered. It has been reported that to successfully grow single grain Nd123 with superior superconductor properties, the fabrication process should be conducted under reduced oxygen partial pressure.[9,10]

Single crystals of Nd-doped Y123 can exhibit high critical current density while proven to be less complicated to fabricate. In earlier studies, it was observed that addition of Nd_2O_3 to Y123 resulted in a significant improvement of the magnetic properties and J_c values up to 8×10^4 A/cm^{-2}.[11,12] Melt textured single crystals of Y123 with <1 mol% Nd_2O_3 have been successfully fabricated.[13]

While most studies in Nd-doped Y123 systems focused on the effect ion substitution on superconducting properties of the materials, little attention is paid to the role of the microstructural development with respect to the improvement of superconducting properties. The objective of this study is to reveal the effect of Nd and Pt additions on the microstructural development of Y123 superconductors processed by top-seeded melt texturing method.

2. Experimental procedure

Nd-doped Y123 samples were processed by the top-seeded melt-texturing technique. The starting compositions of the pellets were Y123 + 0.7 mol% Y211 + 0.1 mol% Nd + 0.2 wt.% PtO, Y123 + 0.7 mol% Y211 + 0.25 mol% Nd + 0.2 wt.% PtO and Y123 + 0.7 mol% Y211 + 0.5 mol% Nd + 0.2 wt.% PtO obtained from Praxair Specialty Ceramics, Woodinville, WA.

The powders were uniaxially pressed to obtain compacts with 13 mm diameter under a pressure of 100 MPa. A Sm123 crystal was placed on the top center of each pellet as a seed for solidifi-

* Corresponding author. Tel.: +1 573 341 7130; fax: +1 573 341 6934.
E-mail address: doganf@mst.edu (F. Dogan).

0955-2219/$ – see front matter © 2008 Elsevier Ltd. All rights reserved.
doi:10.1016/j.jeurceramsoc.2008.01.011

cation of Y123. The powder compacts were placed on substrates made of barium zirconate and heated from room temperature to 1050 °C with the heating rate of 47 °C/h and held at 1050 °C for 0.5 h. The samples were cooled rapidly to 1010 °C, followed by slow cooling between 1010 and 990 °C at a rate of 0.3 °C/h.

A thermal analysis of the Nd–Y123 powders was conducted under a flowing air atmosphere using Netzsch STA 409C/CD. The measuring temperatures ranged from room temperature to 1100 °C. The decomposition temperatures of the powders were determined as the onset of the differential thermal analysis (DTA) curves. Composition and preferred orientation of the single crystal samples were investigated by X-ray diffraction (Scintag XDS 2000 Diffractometer), over angles ranging from 10° to 90° in 2θ. Textured samples were characterized by analyzing of X-ray pole figures (Phillips X-Pert). Elemental compositions and microstructure of the samples were revealed by energy dispersive X-ray spectroscopy and scanning electron microscopy (SEM JEOL-T330A and Hitachi 4700 FESEM) techniques. The size distribution of Y211 particles were determined using Scion Image Software.

3. Results and discussion

The effect of Nd additions on the lattice parameters of the Y123 crystals was determined from the position of the X-ray diffraction peaks. X-ray diffraction of Y123 powders with various Nd concentrations was performed in the range of 2θ between 20° and 60° to analyze the peak shift of (0 0 3), (0 0 5) and (0 0 6) reflections. Shown in Fig. 1, it was observed that a minor peak shift occurred with increasing amount of Nd addition. It is revealed that the *c*-axis lattice parameter of the Y123 increased from 1.16796 to 1.17077 nm as the Nd concentration increased from 0.1 to 0.5 mol%, as shown in Fig. 2. The results suggested that Nd addition resulted in a slight expansion of the *c*-axis lattice parameter.

The increase of lattice parameters (*c*) with increasing Nd concentration from 0.1 to 0.5 mol% may be attributed to the substitution of the Nd^{3+} ions into Y^{3+} sites. Since the ionic radii of Nd^{3+} is larger in comparison to that Y^{3+}, the lattice parameters of the material can be expanded when the substitution of Y^{3+} by Nd^{3+} occurs. A similar observation has also been reported by Schetzle et al.[14]

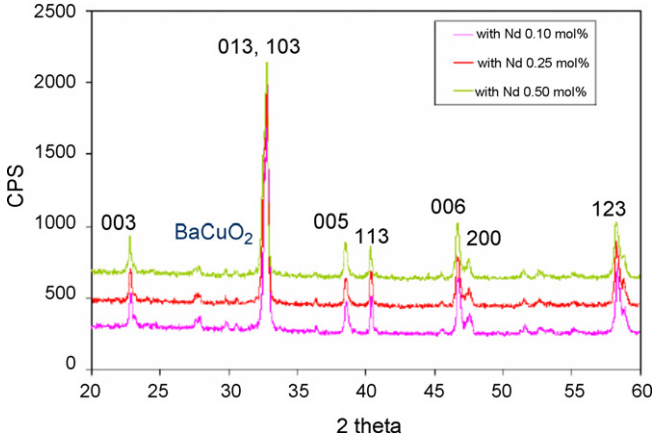

Fig. 1. X-ray diffraction pattern of Y123 powder with different amounts of Nd addition.

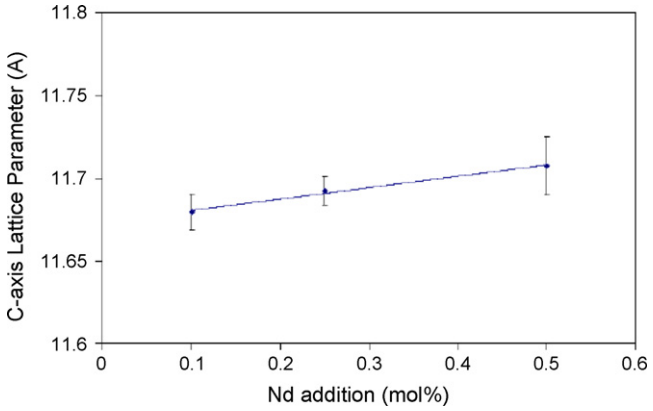

Fig. 2. Dependence of lattice parameters of Nd-doped Y123 compounds on the amount of the Nd addition.

Peritectic decomposition temperature of the samples is one of the factors that strongly affect the solidification process of oxide superconductors. To enhance the crystal growth of Y123, the heating schedule of the melt-texturing process needs to be adjusted according to the decomposition temperature. Fig. 3 shows the differential thermal analysis curves of the samples with various amounts of Nd addition. The DTA results reveal endothermic reactions at two temperature ranges. The major reaction, occurred in the temperature range from 1000 to 1050 °C, representing the peritectic decomposition of Nd–Y123. On the other hand, the minor reaction, representing the dissolution of Nd–Y211 phase, occurred in the temperature range from 920 to 960 °C.

In general, the peritectic decomposition temperature of a doped sample is higher than that of an undoped material. Experimental results from this study exhibited the same trend—the decomposition temperatures of the Nd–Y123 samples increased with increasing amounts of Nd addition. The decomposition temperature of the undoped Y123 sample was found to be 1000.2 °C, while the decomposition temperature of Y123 with 0.5 mol% Nd was 1004.9 °C. Along with the increase of the peritectic decomposition temperatures, Nd additions also affected dissolution of Nd–Y211 particles. DTA results indicate that the dissolution temperature of Nd–Y211 increases from

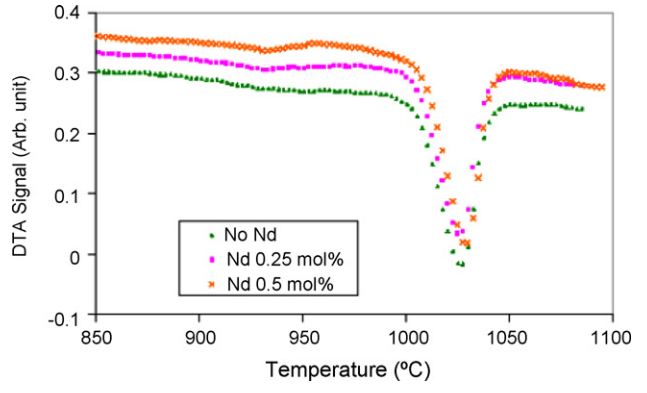

Fig. 3. DTA profile of Nd–Y123 samples with various amount of Nd addition.

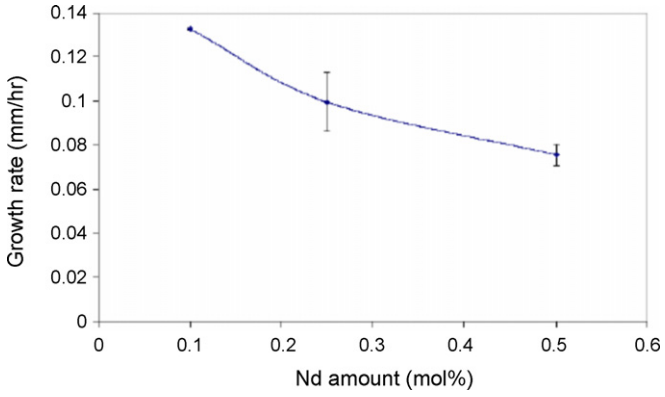

Fig. 4. Average solidification (growth) rate as a function of Nd doping.

928.9 to 932.9 °C as the Nd concentration increases from 0.1 to 0.5 mol%.

The influence of Nd addition on the crystal growth behavior of melt textured Nd–Y123 samples was examined. It was observed that the solidification rate of Nd–Y123 samples slightly decreased as the concentration of Nd increased as shown in Fig. 4. Decrease of the solidification rate in the samples with higher Nd concentration may be attributed to the increase in the peritectic decomposition temperature of the Nd–Y123 samples and the increase in the dissolution temperature of the Nd–Y211 particles.

It was observed that addition of Nd resulted in an increase of the peritectic temperature (T_p) of the Y123 samples as discussed previosly. The enhancement of T_p could lead to reduction of undercooling (ΔT), which strongly relates to the solidification rate. According to the following equation[15]:

$$G = C(\Delta T)n$$

where G is the Y123 growth rate, ΔT the undercooling, which is defined by the difference between the growing temperature and the peritectic temperature, and c and n are constant, a lower undercooling can result in a slower crystal growth.

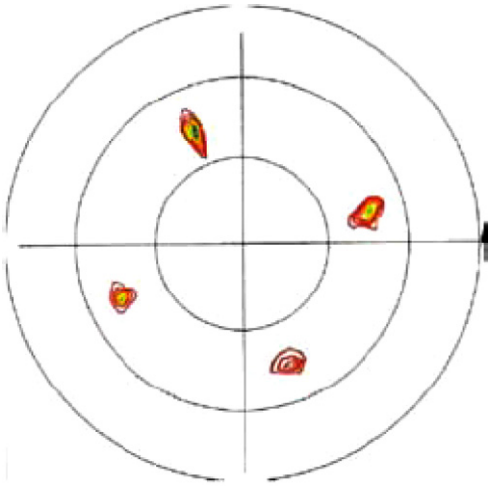

Fig. 5. XRD pole figure from a surface of melt-textured Y123 sample doped with 0.1 wt.% Nd.

Since the superconducting properties of Y123 are strongly related to microstructural development, highly textured samples are desirable. Melt textured Nd–Y123 crystals were grown as square-shaped single grains with the *ab*-plane of the grain lying parallel to the *ab*-plane of the seed. The texture characteristic of the Nd–Y123 crystal was confirmed by the pole figure shown in Fig. 5. The X-ray pole figure exhibited a fairly symmetrical angular distribution of the poles with only minor elongation in azimuth. The result indicated that the sample has a good in-plane texture.

Microstructural development, specifically Nd–Y211 morphology, of the samples is shown in Fig. 6. SEM micrographs indicate that the size and morphology of the Y211 particles are not influenced by the Nd concentration. Needle shaped Nd–Y211 particles with relatively high aspect ratio were observed within the Nd–Y123 matrix in all samples. Average size of Nd–Y211 particles were 1.27, 1.47, and 1.45 μm in the samples with 0.1, 0.25 and 0.5 mol% Nd, respectively. The negligable differences in size of the Nd–Y211 inclusions of samples with varied Nd additions suggest that the refinement of Nd–Y211 are due to platinum present in the starting powder.

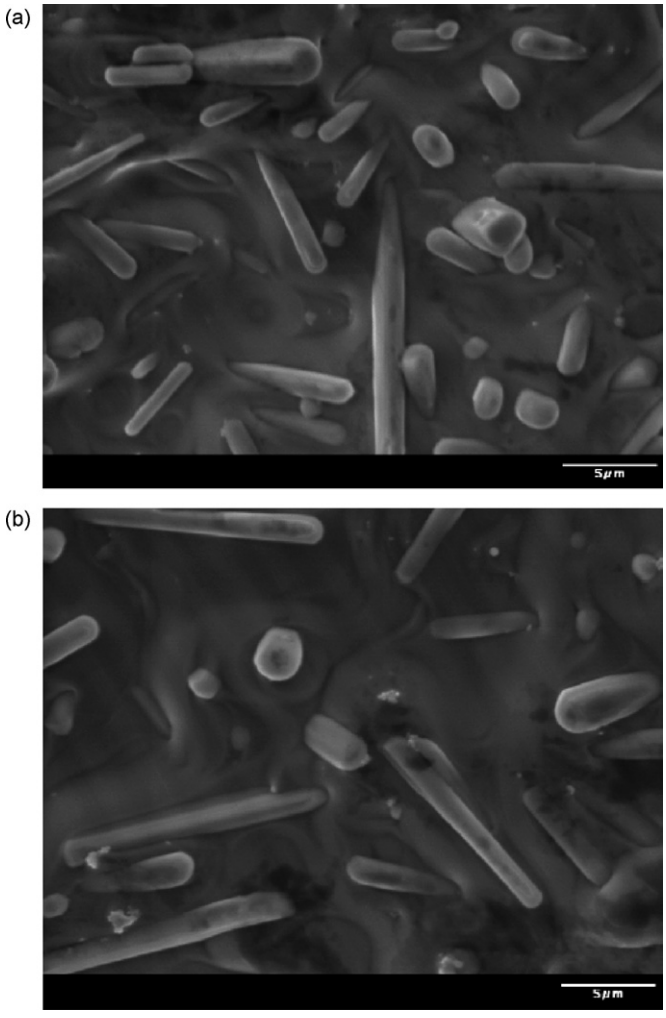

Fig. 6. SEM micrographs showing Y211 size and morphology in samples with Nd addition of 0.1 mol% (a) and 0.25 mol% (b).

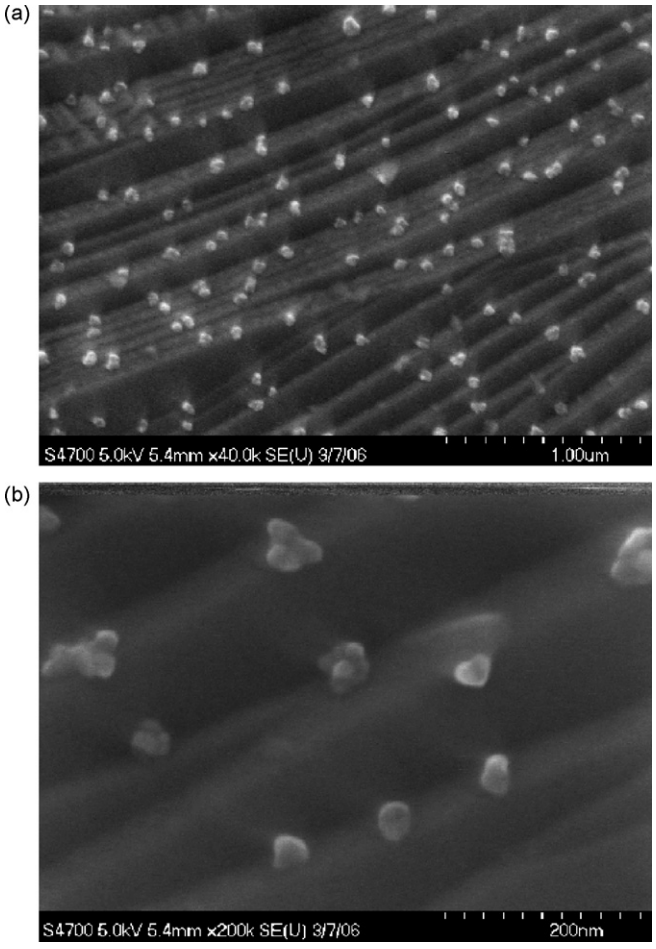

Fig. 7. High magnification SEM micrographs showing nanosized particles within Y123.

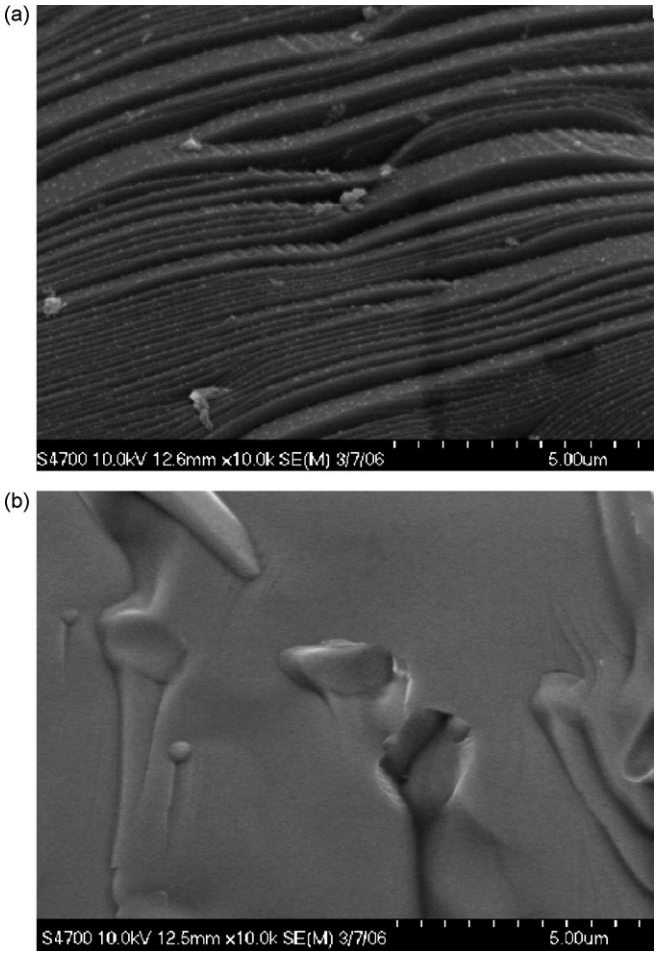

Fig. 8. SEM micrographs showing the region with (a) and without (b) nanosized particles in Y123 matrix.

In addition to the Nd–Y211 particles, SEM micrographs of the samples with Nd additions exhibited precipitated particles embedded in the Nd–Y123 matrix. Fig. 7a and b revealed the faceted crystal habit of the Nd–Y123 matrix. The stair-like morphology of the Nd–Y123 indicate that solidification of Nd–Y123 was controlled by the interfacial kinetics; specifically screw dislocation assisted growth.[15] Nanosized particles embedded in the Nd–Y123 crystal were bright in contrast with particle sizes ranging from 30 to 60 nm.

To identify the elemental composition of the nano-sized precipitates, the SEM equipped with the energy dispersive X-ray spectroscopy (EDS) was utilized. Since the lateral resolution of the EDS was in the micrometer range, which is much larger than the size of the precipitates, it is impractical to precisely determine the composition of nanosized particles by conducting a spot analysis on a single particle. To estimate the elemental composition of nanosized particles, the regions, where nanosized particles were present or absent (Fig. 8a and b), were chosen for compositional analysis. Quantitative analysis from the EDS spectra (shown in Fig. 9a and b) indicated that both regions contained comparable amounts of Y, Ba, Cu, O and Nd. However, platinum was depleted in the region free of nanosized particles (Fig. 8b). Table 1 shows that the platinum content in the region with high-density nano-particles is 0.13 at.%, while platinum is not detected in the region where nano-particles are not observed. The results suggest that the nanosized particles are platinum containing inclusions. It has been reported that addition of platinum in Y123 system typically results in the formation of the $Ba_4CuPt_2O_9$ compound.[16]

Table 1
Elemental compositions of the regions with and without nanosized particles

Element	Composition (at.%)	
	With nanosized particles	Without nanosized particles
O	52.99	52.32
Cu	24.51	24.60
Y	7.03	8.26
Pt	0.13	0.00
Ba	13.09	12.65
Nd	2.26	2.18

Results from the microstructural analysis suggested that the presence of Nd in Y123 may play a role in controlling the size of platinum based inclusions. It has been observed that addition of platinum in Y123 samples could lead to the formation of clustered $Ba_4CuPt_2O_9$ particles. However, the size of the $Ba_4CuPt_2O_9$ clusters was in the range of hundreds of micrometers.[16] On the other hand, nanosized platinum-

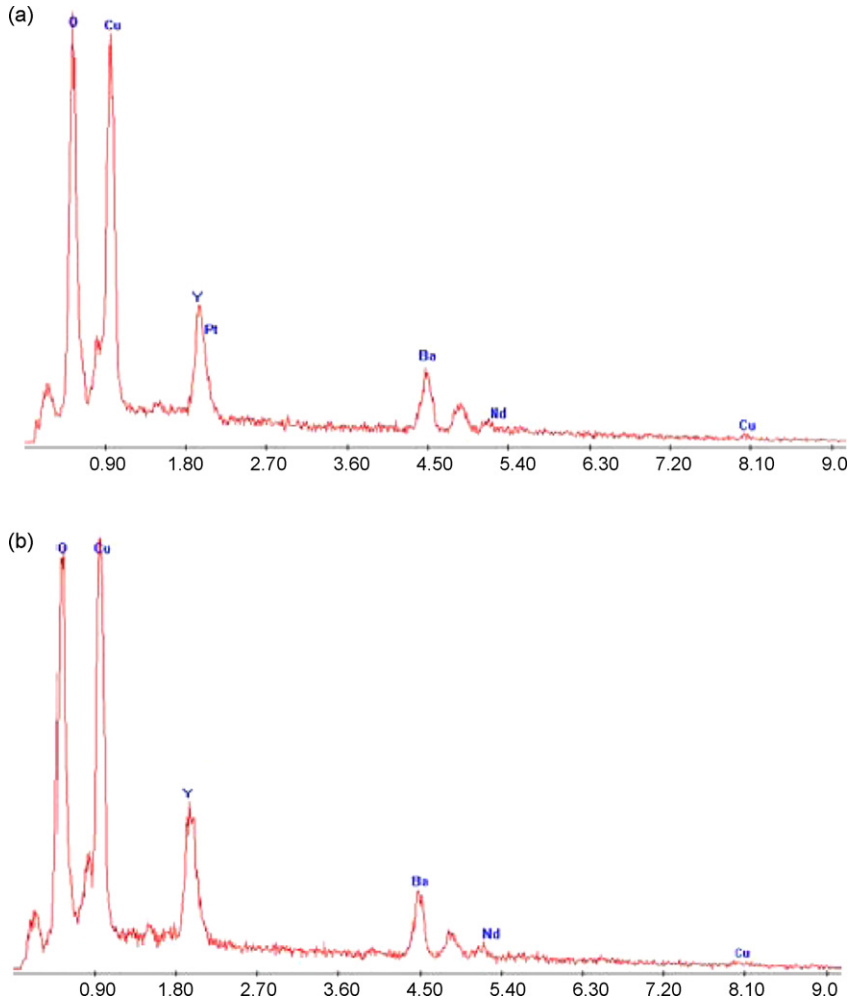

Fig. 9. EDS spectra showing the region with (a) and without (b) nanosized particles.

containing inclusions as well dispersed particles were observed in the Nd–Pt–Y123 system as shown in Fig. 7.

It is well known that the interfaces between the superconducting matrix and the second phase inclusions can act as flux pinning sites in Y123 superconductor. Large amounts of well-dispersed, fine particles lead to an increase of the flux pinning properties. Since melt textured Y123 with Nd addition revealed uniformly distributed nanosized inclusions, higher density of flux pinning sites and enhancement of critical current density can be expected. Enhancement of the flux pinning capacity in Nd-doped Y123 has been reported previously.[13] The maximum trapped field in Y123 magnetized under 0.5 T of Y123 could increase as high as 20% with addition of Nd. It was shown that the maximum trapped field of undoped Y123 crystals was 0.245 T, while the maximum trapped field ranging from 0.26 to 0.295 T was observed in the Y123 with 0.1–0.5 mol% Nd. In addition, an improvement of the critical current density was observed in Nd–Y123 single crystals as compared to that of the undoped Y123. Addition of Nd in the Y123 superconductor could result in the enhancement of the critical current density more than twofold under zero magnetic field. An improvement of the critical current density values up to 1.6×10^4 A/cm^{-2} was observed in Nd–Y123 samples.[13] The results of the present study indicate that the nanosized secondary phase particles may contribute to the enhancement of the critical current density in Y123 system.

4. Summary

Nd and Pt doped Y123 superconducting single crystals were processed my top-seeded melt texturing process. Solidification rate of Nd-doped Y123 was slower than that of undoped compositions. It was shown that nanosized Pt-containing particles were obtained in Nd-Y123 matrix. Refinement of these inclusions which contributed to improvement of superconducting properties such as trapped magnetic field and critical current density, was attributed to Nd-doping of Y123.

Acknowledgements

This work was supported by Boeing Phantom Works and the Materials Research Center at the Missouri University of Science and Technology.

References

1. Campbell, A. M. and Cardwell, D. A., Bulk high temperature superconductors for magnet applications. *Cryogenics*, 1997, **37**, 567–575.
2. Nariki, S., Seo, S. J., Sakai, N. and Murakami, M., Superconducting properties of (Gd, Nd)–Ba–Cu–O bulk superconductor fabricated by melt processing in air. *Supercond. Sci. Technol.*, 2000, **13**, 774–777.
3. Shannon, R. D., Revised effective ionic radii and systematic studies of interatomic distances in halides and chalcogenides. *Acta Crystallogr. A*, 1976, **32**, 751–767.
4. Osabe, G., Yoo, S. I., Sakai, N., Higuchi, T., Takizawa, T., Yasohama, K. *et al.*, Confirmation of Ba-rich $Nd_{1+x}Ba_{2-x}Cu_3O_{7-\delta}$ solid solutions. *Supercond. Sci. Technol.*, 2000, **13**, 637–640.
5. Muralidhar, M., Jirsa, M., Sakai, N. and Murakami, M., Progress in melt-processed (Nd–Sm–Gd)$Ba_2Cu_3O_y$ superconductors. *Supercond. Sci. Technol.*, 2003, **16**, R1–R16.
6. Wu, H. and Wang, S. S., Flux pinning mechanism for Nd–Ba–Cu–O superconductor. *IEEE Trans. Appl. Supercond.*, 1999, **9**, 2211–2214.
7. Zhang, K., Dabrowski, B., Segre, C. U., Hinks, D. G., Hichuller, I. K., Jorgenson, J. D. *et al.*, Solubility and superconductivity in RE $(Ba_{2-x}RE_x)Cu_3O_{7+\delta}$ systems (RE = Nd, Sm, Eu, Gd, Dy). *J. Phys. C*, 1987, **20**, L935–L940.
8. Yoo, S. I. and McCallum, R. W., Phase diagram in the Nd–Ba–Cu–O system. *Physica C*, 1993, **210**, 147–156.
9. Yoo, S. I., Murakami, M., Sakai, N., Higuchi, T. and Tanaka, S., Enhanced flux pinning in melt-processed $NdBa_2Cu_3O_y$ superconductors. *Jpn. J. Appl. Phys.*, 1994, **33**, L1000–L1003.
10. Babu, N. H., Lo, W., Cardwell, D. A. and Shi, Y. H., Fabrication and microstructure of large grain Nd–Ba–Cu–O. *Supercond. Sci. Technol.*, 2000, **13**, 468–472.
11. Matthews, D. N., Cochran, J. W. and Russell, G. J., Melt-textured growth and characterization of a (ND/Y)$Ba_2Cu_3O_{7-\delta}$ composite superconductor with very high critical current density. *Physica C*, 1995, **249**, 255–261.
12. Varanasi, C., Banerjee, A., Yeung, S. and McGinn, P. J., Melt processing of $YBa_2Cu_3O_{7-x}$ with Nd additions. In *High Temperature Superconductors: Synthesis, Processing, and Large-Scale Applications*, ed. U. Balachandran, P. J. McGinn and J. S. Abell. Metals and Materials Society Structural Materials Division Minerals, Warrendale, 1996, pp. 249–259.
13. Dogan, F., Sofie, S. W., Hicks, C., Strasik, M., McCrary, K. E. and Day, A. C., Neodymium oxide doped melt textured $YBa_2Cu_3O_{7-X}$ single crystals. *IEEE Trans. Appl. Supercond.*, 2003, **13**, 3076–3078.
14. Schätzle, P., Bieger, W., Wiesner, U., Verges, P. and Krabbes, G., Melt processing of (Nd, Y)BaCuO and (Sm, Y)BaCuO composites. *Supercond. Sci. Technol.*, 1996, **9**, 869–874.
15. Shiohara, Y. and Endo, A., Crystal growth of bulk high-T_c superconducting oxide materials. *Mater. Sci. Eng. R*, 1997, **19**, 1–86.
16. Dogan, F., Continuous solidification of $YBa_2Cu_3O_{7-x}$ by isothermal undercooling. *J. Eur. Ceram. Soc.*, 2005, **25**(8), 1355–1358.